Case for quasinuclear $\bar{N}N$ bound states

Carl B. Dover
Physics Department, Brookhaven National Laboratory, Upton, New York 11973

T. Gutsche and A. Faessler
Institut für Theoretische Physik, Universität Tübingen, Auf der Morgenstelle 14, 7400 Tübingen, Federal Republic of Germany

(Received 18 July 1990)

Recent experimental results on nucleon-antinucleon annihilation reactions of the type $\bar{N}N \to \pi X$ have provided evidence for a new mesonic state X_2 with quantum numbers $J^{\pi C}(I^G)=2^{++}(0^+)$ which lies outside of the usual quark-antiquark ($Q\bar{Q}$) tensor meson nonet of flavor SU(3). We show that the observed production rates of X_2 from atomic $\bar{p}p$ states of orbital angular momentum $L=0,1$, as well as the decay characteristics of X_2, namely, its preference for $\rho\rho$ over $\pi\pi$ decay and the absence of an observable $\bar{K}K$ mode, are consistent with an interpretation of X_2 as a quasinuclear bound state of the $\bar{N}N$ potential. The principal binding mechanism for such states is provided by the coherent tensor forces for isospin $I=0$ which arise from meson exchanges. We review the evidence for the $0^{++}(0^+)$ and $1^{--}(0^-)$ states predicted in this model and apply the $^3P_0$ strong-coupling quark model to estimate the decay branching ratios for a variety of $\bar{N}N$ bound states. Key experimental tests of our interpretation are discussed.

I. INTRODUCTION AND MOTIVATION

The nucleon-antinucleon ($\bar{N}N$) system provides an excellent entrance channel for the production of a new species of mesons, beyond the well-known quark-antiquark ($Q\bar{Q}$) states which fill the SU(3) nonets of pseudoscalar (spin-parity–charge-parity $J^{\pi C}=0^{-+}$), vector (1^{--}), axial vector (1^{++}), or tensor (2^{++}) mesons. These new mesons might include four quark ($Q^2\bar{Q}^2$) "baryonium" states,[1,2] hybrids ($Q\bar{Q}g$) involving a transverse electric (TE) or magnetic (TM) excitation g of the gluon field,[3–5] excitations of the gluonic fields of quantum chromodynamics ("glueballs"[6–9]), or quasinuclear (QN) bound states of the $\bar{N}N$ potential.[10–14] The latter are analogous to the "quasimolecular" structures which have been invoked to interpret resonance phenomena close to hadronic thresholds [for instance, $\bar{K}K$ (Ref. 15)]. The excitement generated in the 1970s by the possible existence of *narrow* (decay widths $\Gamma \lesssim 20$ MeV/c^2) "baryonium" states coupled to the $\bar{N}N$ system has been dissipated by the nonobservation of such narrow states in a number of precision experiments[16–18] at the Low Energy Antiproton Ring (LEAR) facility at CERN. However, the theoretical arguments[2,19] for narrow baryonium relied on the operation of topological selection rules whose effect was to suppress the direct decay of certain baryonium states into mesons. In other dynamical scenarios, for instance $\bar{N}N$ potential models, only rather broad (typical widths $\Gamma \approx 100$ MeV/c^2) states were anticipated, except in special cases. The focus of this article is on such broad mesonic states, namely, their formation in $\bar{N}N$ annihilation and other hadronic processes, and their expected quantum numbers and decay modes.

Recently, there have been a variety of experiments suggesting the existence of new mesons which cannot be fit into the usual $Q\bar{Q}$ nonets of SU(3). These include studies of $\pi^- p$ interactions[20–24] in which broad mesons with quantum numbers $J^{\pi C}(I^G)=1^{--}(1^+)$ and $1^{-+}(1^-)$ have been seen,[20,21] which couple to the $\pi\phi$ ($l=1$) and $\pi\eta$ ($l=1$) decay channels, respectively (l is the relative orbital angular momentum of the meson-meson system). The 1^{-+} system[21] is "$J^{\pi C}$ exotic," with no coupling to $Q\bar{Q}$. Evidence for new broad mesons X has also been obtained in $\bar{N}N \to \pi X$ (Refs. 25–29) and $\bar{N}N \to \pi\pi X$ (Refs. 30 and 31) reactions from initial quasiatomic $\bar{N}N$ states of orbital angular momentum $L=0$ or 1.

The central thesis of the present article is that the long-predicted nucleon-antinucleon QN bound states with isospin $I=0$ and $J^{\pi C}=0^{++}$, 1^{--}, 2^{++}, which owe their strong binding to the coherent action of tensor forces[12,32] generated by pseudoscalar and vector meson exchanges, have indeed been seen (2^{++}) or strongly hinted at (0^{++}, 1^{--}) as products of $\bar{N}N$ annihilation reactions.[25–30] We justify the case for the existence of QN $\bar{N}N$ bound states by a detailed analysis of the experimental situation, confronting theoretical predictions of production rates[14] and decay branching ratios of QN states with the data.

The outline of the paper is as follows. In Sec. II, we provide a resume of the data which point to the existence of new broad mesons in $\bar{N}N$ annihilation. The best candidate, which is seen in its $\pi^+\pi^-$,[25,29] $\pi^0\pi^0$,[25] and $\rho^0\rho^0$ (Refs. 26–28) decay modes in different experiments, has been assigned quantum numbers $J^{\pi C}(I^G)=2^{++}(0^+)$.

In Sec. III, we review the properties of the $\bar{N}N$ spectrum in potential models[13] and compare the level order, level spacings, isospin degeneracy, etc., with that anticipated for $Q^2\bar{Q}^2$, $Q\bar{Q}g$, or pure glue systems. The $\bar{N}N$ spectrum is characterized by an isoscalar natural parity band (0^{++}, 1^{--}, 2^{++}) of deeply bound states, plus a few

other isovector and/or s-wave bound states closer to the $\bar{N}N$ threshold. The level spacings and isospin properties of $\bar{N}N$ states are distinct from those of $Q^2\bar{Q}^2$, for instance. The $2^{++}(0^+)$ meson seen in $\bar{N}N$ annihilation is interpreted as the $^{13}P_2$-$^{13}F_2$ bound state of the $\bar{N}N$ system.[33] The observed mass and width of this state are shown to be in accord with theoretical estimates. We also examine various $Q^2\bar{Q}^2$ interpretations[34,35] of this state, as well as explanations in terms of meson-meson interactions.[36]

The production of QN states X in annihilation reactions $\bar{N}N \to \pi X$ or γX is the subject of Sec. IV. For the $2^{++}(0^+)$ state X_2, the branching ratio for

$$\bar{N}N(L=1) \to \pi X_2(l=1)$$

is predicted to be considerably enhanced relative to

$$\bar{N}N(L=0) \to \pi X_2(l=2) ,$$

a feature seen in the data. The absolute rates predicted by the $\bar{N}N$ potential are also in agreement with experiment. For QN states lying close to the $\bar{N}N$ threshold, the reaction $\bar{N}N \to \gamma X$ is promising in some cases. However, one must look at exclusive final states; the QN states are too broad to be revealed in the inclusive γ spectrum.

The decay branching ratios of $\bar{N}N$ QN states X are discussed in Sec. V. We estimate the relative rates for quasi-two-body (QTB) decays $X \to M_1 M_2$ in the nonrelativistic quark model, using a version of the $^3P_0$ model[37] which has been successfully applied to meson decay and $\bar{N}N$ annihilation.[38–40] For the decays of X_2, we predict that the $\rho\rho$ decay mode is largest, with a substantial $\pi\pi$ but very small $\bar{K}K$ branch. This is in accord with the observed decay pattern.[25,26] A measurable rate for $X_2 \to \eta\eta$ is also predicted; this would be accessible via a study of the $\bar{p}p \to \pi^0\eta\eta$ reaction.

In Sec. VI, we discuss the key experimental signatures which would provide justification of the hypothesis of $\bar{N}N$ quasinuclear states advanced here. The experimental study of $\bar{N}N$ annihilation channels involving only neutral mesons ($3\pi^0$, $\pi^0\pi^0\eta$, $\pi^0\eta\eta$, 3η, for example), will be particularly important in the search for $\bar{N}N$ and other more exotic mesons.

II. EXPERIMENTAL DATA

Recently, the ASTERIX group at LEAR investigated the $\bar{p}p \to \pi^0\pi^+\pi^-$ reaction initiated from an $L=1$ atomic state (L is the relative orbital angular momentum of the $\bar{N}N$ system). They found a peak in the $\pi^+\pi^-$ mass spectrum at 1565 MeV, as displayed in Fig. 1. From a decay analysis and the absence of a similar peak in the $\pi^\pm\pi^0$ spectrum, the quantum numbers are assigned to be[29]

$$J^{PC}(I^G) = 2^{++}(0^+) \text{ for } X_2(1565) . \tag{2.1}$$

We introduce the notation X_J for the states of spin J discussed here; note that $X_2(1565)$ corresponds to the $AX(1565)$ of May *et al.*,[29] which we will later identify with the $0^{++}(0^+)$, $1^{--}(0^-)$, $2^{++}(0^+)$ members of a band of isoscalar, natural-parity $\bar{N}N$ bound states. The production branching ratio B is found to be[29]

$$B(\bar{p}p(L=1) \to \pi^0 X_2) B(X_2 \to \pi\pi) \approx (5.6 \pm 0.9) \times 10^{-3} . \tag{2.2}$$

Here we have used

$$B(X_2 \to \pi\pi) = B(X_2 \to \pi^0\pi^0) + B(X_2 \to \pi^+\pi^-)$$

and

$$B(X_2 \to \pi^+\pi^-) = 2B(X_2 \to \pi^0\pi^0)$$

for the decay of an isospin $I=0$ meson to obtain Eq. (2.2) from the measured value for $\pi^+\pi^-$ decay given in Table I.

In earlier bubble-chamber experiments (dominated by $L=0$ $\bar{N}N$ annihilation), Gray *et al.*[25] saw evidence for a peak at around 1530 MeV in the $\pi^+\pi^-$ and $\pi^0\pi^0$ spectra from $\bar{p}n \to 2\pi^-\pi^+$ and $\bar{p}p \to 3\pi^0$ annihilation. The $\pi^+\pi^-$

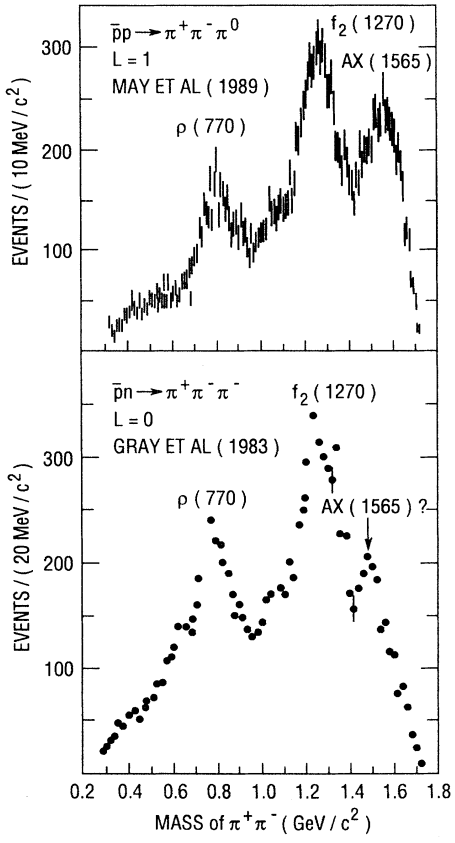

FIG. 1. Mass spectrum of the $\pi^+\pi^-$ system produced in nucleon-antinucleon annihilation into three pions. The spectrum of May *et al.* (Ref. 29) refers to annihilation from the atomic p state ($L=1$). The peak corresponding to the formation of the $AX(1565)$ [a $2^{++}(0^+)$ meson] is clearly seen. The $\bar{p}n$ annihilation data, from the $\bar{p}d$ experiment of Gray *et al.* (Ref. 25), are shown at the bottom; here the annihilation is mostly s wave ($L=0$). A peak in the mass region of the $AX(1565)$ is also evident in the $L=0$ data. Note that hint of a structure X_0 near 1100 MeV at the same mass as $\pi^+\pi^-$ enhancements seen in $\bar{p}n \to \rho^- X_0$ (Ref. 30), $\bar{p}p \to \rho^0 X_0$ (Ref. 45), and $\bar{p}p \to \omega X_0$ (Ref. 44).

TABLE I. Candidates for $\bar{N}N$ bound states X.

Mass (MeV/c^2)	Width (MeV/c)	Reaction	Branching ratio[a]	Reference
1480	120	$\bar{p}n \to \pi^- X$, $X \to \rho^0\rho^0$	$(3.7\pm0.3)\times10^{-2}$	Bridges *et al.*[26,27]
1500[b]	200	$\bar{p}n \to \pi^- X$; $X \to 2\pi^+2\pi^-$	not given	Ahmad *et al.*[28]
1530	100	$\bar{p}n \to \pi^- X$; $X \to \pi^+\pi^-$	$(2.6\pm0.4)\times10^{-3}$	Gray *et al.*[25]
		$\bar{p}p \to \pi^0 X$; $X \to \pi^0\pi^0$	$(1.6\pm0.5)\times10^{-3}$	
		$\bar{p}n \to \pi^- X$; $X \to K^+K^-$	$\leq 1.1\times10^{-4}$	
		$\bar{p}n \to \pi^- X$; $X \to K_SK_S$	$\leq 0.4\times10^{-4}$	
		$\bar{p}p \to \pi^0 X$; $X \to K_SK_S$	$\leq 0.9\times10^{-4}$	
1565	170	$\bar{p}p \to \pi^0 X$; $X \to \pi^+\pi^-$	$(3.7\times0.6)\times10^{-3}$	May *et al.*[29]
1250	150	$\bar{p}p \to \pi^0 X$; $X \to e^+e^-$	very few events	Bassompierre *et al.*[41]
1110	110	$\bar{p}n \to \rho^- X$; $X \to \pi^+\pi^-$	$(2.4\pm0.4)\times10^{-2}$	Daftari *et al.*[30]

[a]The cited branching ratios include only the charge state listed.
[b]We give the mass and width values corresponding to the data with low proton spectator momentum; for higher spectator momenta, the peak shifts to lower mass.

spectrum for the former reaction is shown in Fig. 1. Recently, evidence for the $AX(1565)$ in the $\pi^0\pi^0$ decay channel has been obtained by the Crystal Barrel Collaboration at LEAR.[70] The masses and widths obtained are sensitive to the shape of the assumed continuum background in the 3π channel, as well as the parametrization of the other quasi-two-body channels (here $\pi\rho$ and πf) which contribute. For instance, Gray *et al.*[25] allow the width of the $f(1270)$ meson to be a free parameter in fitting the 3π spectrum, while May *et al.*[29] do not follow this procedure. These different fit procedures could account for the somewhat different masses obtained for the $\pi\pi$ resonance X_2 as seen in $L=0$ and 1 annihilations. In Table I, we have given masses and widths to the nearest 10 MeV; the uncertainties in these values due to the use of different prescriptions for treating the QTB and continuum contributions are likely to be larger than the statistical uncertainties generated by the fit, so we do not cite the latter values. It is very probable that the $AX(1565)$ meson seen by May *et al.*[29] and the $f_2'(1530)$ detected earlier by Gray *et al.*[25] are one and the same object. We assume this identity here [$AX(1565)=f_2'(1530)\equiv X_2$]. From Table I, we have[25]

$$B(\bar{p}n \to \pi^- X_2)B(X_2 \to \pi\pi) \approx (3.9\pm0.6)\times10^{-3} , \quad (2.3a)$$

$$B(\bar{p}p\,(L=0) \to \pi^0 X_2)B(X_2 \to \pi\pi) \approx (4.7\pm1.4)\times10^{-3} , \quad (2.3b)$$

or

$$B(\bar{p}p\,(L=0) \to \pi^0 X_2)/B(\bar{p}n \to \pi^- X_2) \approx 1.2\pm0.4 . \quad (2.4)$$

Since X_2 is an isoscalar, this ratio should be $\frac{1}{2}$, if the $\bar{p}n$ system is in an $L=0$ state and the initial $\bar{p}p$ atomic state is indeed pure $\bar{p}p$. However, in the neutral atomic state, $\bar{p}p$-$\bar{n}n$ mixing is known to be a significant effect,[14,42] and the ratio (2.4) is strongly model dependent. For instance, the rates are sensitive to the presence of a node in the $^3S_0$ or $^1S_0$ radial wave functions;[14] see also, Eq. (4.5). A phenomenological model for the breakdown of isospin symmetry in $\bar{N}N$ annihilation has recently been developed by Klempt.[42] In addition, Reifenröther and Klempt[42] have provided arguments indicating that two-body $\bar{p}n$ annihilation with $L=1$ is important at rest, even though the $\bar{p}d$ system is dominantly in an s state. It is argued[42] that the small $\bar{p}n$ $L=1$ contribution found by Angelopoulos *et al.*[16] is due to tight cuts on the momentum of the spectator nucleon, which suppresses $L=1$ annihilation from $\bar{p}d$ atomic s states. For $\bar{p}p$, on the other hand, $L=0$ annihilation dominates for a liquid target, so we indicate this in Eq. (2.3b). The presence of $L=1$ $\bar{p}n$ annihilation will also cause the ratio (2.4) to deviate from $\frac{1}{2}$. However, $L=1$ contributions tend to make this ratio *smaller* than $\frac{1}{2}$, so the empirical value in Eq. (2.4) remains difficult to understand.

Further, the $\bar{K}K$ decay mode of X_2 is strongly suppressed,[25] i.e.,

$$B(X_2 \to \bar{K}K)/B(X_2 \to \pi\pi) \leq 1/16 . \quad (2.5)$$

Thus, as noted by Gray *et al.*,[25] X_2 cannot be identified with the well-known $f'(1525)$ meson, an $s\bar{s}$ state which decays dominantly to $\bar{K}K$.

Another $2^{++}(0^+)$ state, decaying into $\rho^0\rho^0$, in the same mass region was found by Bridges *et al.*[26,27] in their analysis of data on the $\bar{p}d \to 3\pi^-2\pi^+p$ reaction at rest (see Table I). The existence of a peak near 1500 MeV in the π^+-π^- difference spectrum was later verified by Ahmad *et al.*;[28] these authors did not provide a quantum number analysis or a branching ratio, however. It was shown[28] that the apparent mass of the state depends on the momentum of the "spectator" proton in $\bar{p}d$ annihilation, with higher spectator momentum being associated with a state of lower mass and larger width. This is a natural effect of final-state interactions of the produced meson with the proton, and has been analyzed quantitatively by Kolybasov *et al.*[43] Thus, we do not view the difference in mass between the $2^{++}(0^+)$ state seen in the $\rho^0\rho^0$ channel near 1480–1500 MeV and the $\pi^+\pi^-$ channel around 1530–1565 MeV to be very significant, due to the effects of final-state interactions and other ambiguities in the analysis. It seems a reasonable hypothesis that the $2^{++}(0^+)$ structures seen in the $\rho^0\rho^0$, $\pi^+\pi^-$, and $\pi^0\pi^0$ final states are, in fact, one and the same object (here

called X_2). If we assume this, we have

$$B(\bar{p}n \to \pi^- X_2) B(X_2 \to \rho\rho) \simeq (11.1 \pm 0.8) \times 10^{-2} . \quad (2.6)$$

In obtaining Eq. (2.6), Bridges *et al.*[26,27] attribute a very large fraction (0.82 ± 0.05) of the $\bar{p}n \to 3\pi^- 2\pi^+$ events,

$$B(\bar{p}n \to 3\pi^- 2\pi^+) \approx (4.5 \pm 0.2) \times 10^{-2} ,$$

to X_2 production. This is probably an overestimate, since their analysis[26,27] did not consider the contribution of QTB modes, particularly $\bar{p}n \to \rho^0 A_1^- (l=0)$. Taken at face value, Eqs. (2.3a) and (2.6) imply

$$B(X_2 \to \rho\rho)/B(X_2 \to \pi\pi) \approx 28.5$$

or (2.7)

$$B(X_2 \to \pi\pi) \leq 3.4 \times 10^{-2} .$$

As we show later, this limit on $B(X_2 \to \pi\pi)$ is not consistent with the observed rate for $\bar{p}p(L=1) \to \pi^0 X_2$ seen at LEAR.[29] However, Eq. (2.7) is sensitive to the fraction of $\bar{p}n(L=1)$ annihilations, which differs in Eqs. (2.3a) and (2.6), due to different momentum cuts on the spectator proton.

In addition to the $2^{++}(0^+)$ state around 1500 MeV in Table I, we also list candidates near 1110 and 1250 MeV which are seen in other $\bar{N}N$ annihilation reactions. The peak at 1250 MeV is not well established, since the sample of e^+e^- events is very sparse. If it is confirmed, it is a candidate to identify with the $1^{--}(0^-)$ $\bar{N}N$ bound state, which we call $X_1(1250)$. Finally, the structure in the $\pi^+\pi^-$ channel[30] near 1110 MeV has also been seen by Bizzarri *et al.*[44] in the $\bar{p}p \to \omega\pi^+\pi^-$ reaction and by Diáz *et al.*[45] in $\bar{p}p \to \rho^0\pi^+\pi^-$. In these papers, the fits to this peak are accomplished by including poles in the s-wave isoscalar $\pi\pi$ amplitude, which corresponds to 0^{++} quantum numbers. The structure near 1110 MeV, which is strongly coupled to the $\bar{N}N$ system due to its formation mechanism, is referred to as $X_0(1110)$.

We emphasize the 0^{++}, 1^{--}, and 2^{++} states of Table I as candidates for $\bar{N}N$ bound states, since they have been seen in $\bar{N}N$ annihilation reactions.[25–30,41] However, one should recall that there are other candidates for 0^{++} and 2^{++} mesons in the same mass region which are not seen in $\bar{N}N$ annihilation. For instance, the $G(1590)$ $[0^{++}(0^+)]$, seen in 100 GeV/c $\pi^- p$ collisions,[24] and observed in $\pi\pi$, $\eta\eta$, and $\eta\eta'$ decay modes, is not seen in J/ψ radiative decays[46] or pp central production, while the $\theta(1690)$ $[2^{++}(0^+)]$ is seen in $\pi^- p$ interactions at 22 GeV/c,[23] J/ψ decays,[46] and pp collisions at 300 GeV/c.[47] The $G(1590)$ and $\theta(1690)$, considered to be glueball candidates, have not yet been seen in $\bar{N}N$ annihilation.

There are also abundant data on two-meson production in the two-photon process $\gamma\gamma \to M_1 M_2$; for a recent review, see Kolanoski.[48] In the channels $\gamma\gamma \to \pi^0\pi^0$, $\pi^+\pi^-$, no indications of $X_0(1110)$ or $X_2(1565)$ are seen; the spectrum is dominated by $f(1270)$ production. In the channel $\gamma\gamma \to \rho^0\rho^0$, a strong enhancement is seen near threshold, while for $\gamma\gamma \to \rho^+\rho^-$, a much smaller cross section is found.[48] Partial-wave analyses[49] suggest mostly 0^{++} strength below 1700 MeV and 2^{++} at larger mass, but this conclusion is not yet definitive. In any case, it is clear that the $\gamma\gamma \to \rho^0\rho^0$ threshold enhancement cannot be attributed to a single $I=0$ resonance [for instance, $X_2(1565)$], since then the enhancement must appear with doubled strength in the $\rho^+\rho^-$ channel, which is not observed. In fact, the essence of the four-quark ($Q^2\bar{Q}^2$) resonance interpretation[50,51] of the $\gamma\gamma \to \rho^0\rho^0$ enhancement is that there exists an essentially degenerate pair of 2^{++} resonances with $I=0,2$ lying near to the $\rho\rho$ threshold, which produce constructive interference in the $\rho^0\rho^0$ channel and destructive interference for $\rho^+\rho^-$. The $Q^2\bar{Q}^2$ model runs into difficulties for the $\gamma\gamma \to \phi\rho^0$ channel, however, predicting a large peak for a $\phi\rho^0$ mass near 2 GeV, contrary to experiment.[48] As we discuss in more detail later, the $Q^2\bar{Q}^2$ and $\bar{N}N$ pictures differ very clearly in their isospin properties. The 0^{++}, 1^{--}, 2^{++}, ..., band of deeply bound $\bar{N}N$ states contains only $I=0$ members, whereas the $Q^2\bar{Q}^2$ spectrum contains a band with degenerate $I=0,1,2$ states composed of a diquark and antidiquark of spin and isospin 1. Note that there is no evidence for $I=2$ mesons in $\bar{N}N$ annihilation. For instance, in the $\bar{p}n \to 2\pi^-\pi^+$ reaction where X_2 is seen, there is no corresponding peak in the $\pi^-\pi^-$ spectrum ($I=2$).

In any case, the $\bar{N}N$ bound states seen in $\bar{N}N$ annihilation reactions will be difficult to detect in $\gamma\gamma$ collisions, because of their multiquark character and their tendency to couple to a number of different meson-meson configurations.

III. SPECTRUM OF $\bar{N}N$ BOUND STATES

A model for the $\bar{N}N$ potential $V_{\bar{N}N}(r)$ due to meson exchanges can be constructed from the nucleon-nucleon potential V_{NN} by the G-parity transformation, i.e.,

$$V_{NN} = \sum_i V_i ,$$
$$V_{\bar{N}N} = \sum_i G_i V_i , \quad (3.1)$$

where G_i is the G parity of meson i, and V_i can be decomposed as

$$V_i = V_c + \boldsymbol{\sigma}_1 \cdot \boldsymbol{\sigma}_2 V_\sigma + \mathbf{L} \cdot \mathbf{S} V_{LS} + S_{12} V_T + Q_{12} V_{LS2} \quad (3.2)$$

in terms of central (V_c), spin-spin (V_σ), spin-orbit (V_{LS}), tensor (V_T), and quadratic spin-orbit (V_{LS2}) contributions, where we define, as usual,

$$Q_{12} = \tfrac{1}{2}(\boldsymbol{\sigma}_1 \cdot \mathbf{L} \boldsymbol{\sigma}_2 \cdot \mathbf{L} + \boldsymbol{\sigma}_2 \cdot \mathbf{L} \boldsymbol{\sigma}_1 \cdot \mathbf{L}) ,$$
$$S_{12} = 3\boldsymbol{\sigma}_1 \cdot \hat{\mathbf{r}} \boldsymbol{\sigma}_2 \cdot \hat{\mathbf{r}} - \boldsymbol{\sigma}_1 \cdot \boldsymbol{\sigma}_2 . \quad (3.3)$$

The general features of the $\bar{N}N$ spectrum in potential models have been discussed by a number of authors.[10–14,32,33,52–56] The key notion in understanding the level order of the spectrum of $\bar{N}N$ bound states and resonances is the *coherence* (like signs) of different components of the meson-exchange potentials in certain quantum states $^{2I+1,2S+1}L_J$ (I is the isospin, S is the spin, L is the orbital angular momentum, and J is the to-

tal angular momentum). These coherences, the most important of which is due to tensor potentials, provide the main characteristics of the $\bar{N}N$ spectrum:

(1) The existence of a natural-parity band of $I=0$, $S=1$, $L=J\pm1$ states ($^{13}P_0$, $^{13}S_1$-$^{13}D_1$, $^{13}P_2$-$^{13}F_2$, ...), supported by the attractive coherence of tensor, quadratic spin-orbit, and vector meson-exchange contributions to the potential.

(2) $I=1$ $\bar{N}N$ states tend to cluster near threshold (mass $2m_N\approx1880$ MeV), due to the absence of strong coherences.

(3) Close-lying isospin doublets can only occur for $S=0$, and only in particular models;[57] isospin degeneracy does not occur for $S=1$, since the strong $\bar{N}N$ tensor interaction produces large isospin splittings for states of the same $\{L,S,J\}$.

These properties of the $\bar{N}N$ spectrum are illustrated in Fig. 2, taken from Refs. 13, 54, and 55. One notes the $I=0$ band of deeply bound states, with

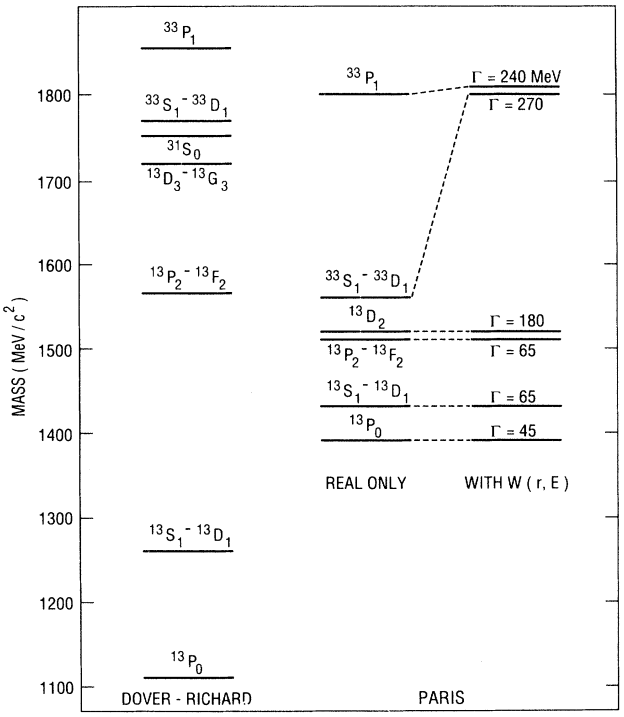

FIG. 2. Predictions for the mass spectrum of nucleon-antinucleon bound states in the framework of a potential model. The real part of the $\bar{N}N$ potential is generated by a G-parity transformation on the meson-exchange part of the NN potential, as per Eq. (3.1). The Dover-Richard spectrum is taken from Ref. 13, and displays the typical level order of nonrelativistic one-boson-exchange models, with a low-lying isospin $I=0$ natural-parity (0^{++}, 1^{--}, 2^{++}) band plus a few $I=1$ states clustered near threshold. This pattern of levels reflects the action of the attractive and coherent tensor potential for $I=0$, $L=J\pm1$. The spectrum labeled PARIS, taken from Refs. 54 and 55, shows the effect of an energy-dependent annihilation potential $W(r,E)$. In this model, the main consequence of absorption is that the $\bar{N}N$ levels acquire a typical hadronic width of order $\Gamma\approx50$–250 MeV.

$$J^{\pi C}(I^G)=[0^{++}(0^+),1^{--}(0^-),2^{++}(0^+),\ldots],$$

plus a sprinkling of $I=1$, $L=0,1$ configurations closer to threshold. Note that there is no reliable estimate for the absolute masses of $\bar{N}N$ states, since the transformation (3.1) is useful only for the medium- and long-range parts of the potential. The short-range behavior of $V_{\bar{N}N}$ is essentially unknown. Thus, for the spectrum labeled Dover-Richard in Fig. 2, an arbitrary square-well cutoff is applied:

$$V_{\bar{N}N}(r)=\begin{cases}\sum_i G_i V_{NN}(r) & \text{for } r\geq r_0\ ,\\ \sum_i G_i V_{NN}(r_0) & \text{for } r\leq r_0\ .\end{cases}\tag{3.4}$$

Here $r_0\approx0.8$ fm is chosen to position to the $2^{++}(0^+)$ state near 1565 MeV/c^2, where the corresponding candidate $\bar{N}N$ state appears in Table I. With this cutoff prescription, the 0^{++} and 1^{--} states also lie close to the $X(1100)$ and $X(1250)$ structures seen in their $\pi^+\pi^-/e^+e^-$ modes, respectively (see Table I).

The meson-exchange potential $V_{\bar{N}N}$ is only part of the story; in addition, one has the annihilation processes $\bar{N}N\to M_1M_2$ or $M_1M_2M_3$, which contribute an additional energy-dependent complex potential $V_A(r,E)+iW(r,E)$ in a one-channel optical-model description. The effects of an energy-dependent absorptive potential $W(r,E)\sim e^{\lambda E}$ ($E\leq0$ for bound states) for $I=0$ states[54] is shown in Fig. 2. The natural-parity 0^{++}, 1^{--}, ..., band is seen to be broadened, without any significant mass shift. An energy-independent $W(r)$, on the other hand, with $V_A=0$, produces a large repulsive mass shift as well as a substantial decay width ($\Gamma\geq200$ MeV) for the $I=1$ $^{33}S_1$-$^{33}D_1$ state. In a microscopic quark rearrangement picture, Niskanen and Green[53] obtained an annihilation potential with a sizeable attractive real part $V_A(r,E)$, leading to additional binding for quasinuclear $\bar{N}N$ states. This model[53] leads to an absorptive part $W(r,E)$ which decreases sharply as the binding energy increases, leading to very narrow ($\Gamma\leq10$–20 MeV) deeply bound 0^{++}, 1^{--}, 2^{++} states. The Paris group,[54,55] with an energy-dependent $W(r,E)$ for $I=0$, predicts widths $\Gamma\approx44$–65 MeV which are also smaller than those in Table I. At its present stage of development, the microscopic quark model[53] yields only about 60% of the observed $\bar{N}N$ annihilation cross section, and hence it is not surprising that it also leads to an underestimate of the annihilation width of bound states. This deficiency is understandable in that only a restricted set of annihilation channels is considered. This class of quark models could be systematically improved in order to obtain better agreement with data.

A rough estimate of the scale of annihilation widths Γ expected for $\bar{N}N$ bound states may be obtained from the semiclassical formula[13]

$$\Gamma\approx v\sigma_A\int_0^\infty dr\,u^2(r)f(r)\ ,\tag{3.5}$$

where $v\sigma_A$ is the annihilation cross section σ_A times relative velocity v (in principle, the imaginary part of an amplitude continued to negative energy), $u(r)$ is the $\bar{N}N$

radial wave function, and the normalized function $f(r)$ represents the spatial extent of the annihilation potential. For $f(r)\sim e^{-r/a}$ and $u(r)$ sharply peaked at $r\approx R_0$, we obtain

$$\Gamma\approx v\sigma_A e^{-R_0/a}/8\pi a^3 . \tag{3.6}$$

Choosing $v\sigma_A\approx 40$ mb, $a\approx 0.3$ fm (corresponding to $\langle r^2\rangle_A^{1/2}\approx 1.05$ fm), we estimate

$$\Gamma\approx 115 \text{ MeV} \quad \text{for } R_0\approx 0.7 \text{ fm} , \tag{3.7}$$

the value of R_0 being typical[13] for a $^{13}P_2$-$^{13}F_2$ state bound by about 300 MeV [near $X_2(1565)$]. Although this perturbative estimate is not accurate, it does indicate that an energy-independent $W(r)=W_0e^{-r/a}$, with $W_0=v\sigma_A/16\pi a^3$ obtained from observed cross sections near threshold, leads to values of Γ not far from those of the experimentally observed states in Table I.

The main dynamical mechanism for producing the 0^{++}, 1^{--}, 2^{++} ($I=0$) band is the coherent tensor interaction (π, η, ρ, ω tensor terms all have the same sign). Unlike the situation for the deuteron, where the $^3S_1$-$^3D_1$ mixing is weak, the $I=0$, $S=1$, $\bar{N}N$ bound states X_J are close to the coherent mixture[32]

$$X_J=(-\sqrt{J}\,|L=J-1\rangle + \sqrt{J+1}\,|L=J+1\rangle)/(2J+1)^{1/2} , \tag{3.8}$$

which diagonalizes the tensor operator S_{12}. For this configuration, the diagonal $\bar{N}N$ potential is of the form

$$\langle X_J|V|X_J\rangle = V_c+V_{\sigma\sigma}-3V_{LS}-4V_T + (J^2+J+4)V_{LS2}+\frac{\hbar^2}{M_N}\frac{(J^2+J+2)}{r^2} , \tag{3.9}$$

where V_c, $V_{\sigma\sigma}$, V_{LS}, V_T, and V_{LS2} are all positive. Inserted in a nonrelativistic bound-state equation, this potential implies an approximate mass formula for the $I=0$ band of rotational form

$$M(X_J)=M(X_0)+\Delta M\ J(J+1) \tag{3.10}$$

and the *interval rule*

$$M(X_2)-M(X_1)\approx 2[M(X_1)-M(X_0)] . \tag{3.11}$$

This rule is well satisfied by the Dover-Richard spectrum in Fig. 2 and continues to hold when annihilation is included as for the spectrum labeled PARIS. The candidate states X_J in Table I are seen to satisfy Eq. (3.11) rather well, so they are consistent with an $\bar{N}N$ band whose binding is dominated by tensor forces.

Let us now contrast the $\bar{N}N$ spectrum with that predicted for four-quark systems ($Q^2\bar{Q}^2$), for instance, by Jaffe.[1] Here, one starts with diquarks α and β of color $\{\bar{3}\}$ with spin-isospin $(S,I)=(0,0)$ and $(1,1)$, respectively. Diquarks with color $\{6\}$ have also been considered;[2] an alternative version of the $Q^2\bar{Q}^2$ model has been recently discussed by Bose and Sudarshan.[35] Jaffe[1] gives three trajectories A, $B^{\pm}$, and C with structure $\alpha\bar{\alpha}$, $\alpha\bar{\beta}\pm\bar{\alpha}\beta$, $\bar{\beta}\beta$, respectively, depicted in Fig. 3. Trajectory A has 0^{++}, 1^{--}, 2^{++} members with $I=0$, identical in quantum numbers to the deeply bound band in the $\bar{N}N$ model (see Fig. 2). Note, however, that the mass formula for $Q^2\bar{Q}^2$ states assumes the form of a Regge trajectory

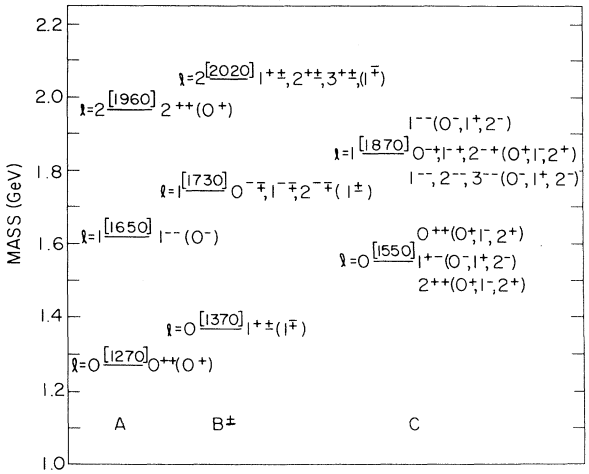

FIG. 3. Mass spectrum of $Q^2\bar{Q}^2$ nonstrange four-quark states, as predicted by Jaffe (Ref. 1). The trajectories A, $B^{\pm}$, and C correspond to configurations $\alpha\bar{\alpha}$, $\alpha\bar{\beta}\pm\bar{\alpha}\beta$, and $\beta\bar{\beta}$, respectively, where the diquarks α and β have color $\{\bar{3}\}$ and spin isospin (0,0) or (1,1). The levels are labeled by the mass in MeV/c^2, the quantum numbers $J^{\pi C}(I^G)$, and the relative orbital angular momentum l between Q^2 and $\bar{Q}^2$.

$$M^2(X_J)=M^2(X_0)+J/\alpha , \tag{3.12}$$

where $\alpha=0.9$ GeV^{-2} is the same as the slope parameter for ordinary $Q\bar{Q}$ trajectories. Clearly, the candidates in Table I cannot be interpreted as Jaffe's $Q^2\bar{Q}^2$ states, since the 2^{++} member is predicted[1] to lie in the $\bar{N}N$ continuum, some 400 MeV above the observed $X_2(1565)$. Secondly, the $Q^2\bar{Q}^2$ interval rule

$$M^2(X_2)-M^2(X_1)=M^2(X_1)-M^2(X_0) \tag{3.13}$$

is quite distinct from Eq. (3.11), and would predict $M(X_1)\approx 1160$ MeV and $M(X_0)\approx 480$ MeV if $M(X_2)$ is fixed at 1565 MeV, an unacceptable result.

Trajectory C of the $Q^2\bar{Q}^2$ spectrum displays a high degree of degeneracy in both spin and isospin. In particular, $I=2$ mesons, absent in the $\bar{N}N$ spectrum, are an essential feature. Liu and Li[34,51] and Achasov[50] have suggested the interference of $2^{++}(0^+)$ and $2^{++}(2^+)$ states as a means of understanding the $\gamma\gamma\to\rho\rho$ data. However, if $X_2(1565)$ is identified as the $2^{++}(0^+)$ state on $Q^2\bar{Q}^2$ trajectory C, then we would also expect to see a $\pi^-\pi^-$ resonance near $X_2(1565)$. There is no evidence for any such $I=2$ state in the $\bar{N}N$ annihilation data.

One could also consider other interpretations of the $X_2(1565)$. The possibility that $X_2(1565)$ is just the $f_2'(1525)$, i.e., the strange-antistrange ($s\bar{s}$) partner of the $f_2(1270)$, is ruled out by Eq. (2.5). The interpretation of $X_2(1565)$ as the radial excitation of $f_2(1270)$ is also unten-

able, since X_2 lies too low in mass. $X_2(1565)$ could contain a component of a gluonic excitation, for instance, a hybrid ($Q\bar{Q}g$) (Refs. 3–5) or glueball (gg).[6–9] The spectroscopy of these objects has been recently reviewed in Ref. 58 by Meshkov, Schierholz, and Godfrey. In lattice gauge calculations, the 0^{++} and 2^{++} glueballs lie lowest in mass, with $M(0^{++})\approx 10\Lambda\sim 1.4$ GeV [Λ is the mass scale of quantum chromodynamics (QCD)] and $M(2^{++})/M(0^{++})\approx\frac{3}{2}$ according to Schierholz.[58] The two-gluon system allows four 2^{++} states, corresponding to $^5S_2$, $^1D_2$, $^5D_2$, and $^5G_2$ combinations. One can make a case that the four 2^{++} candidates,[22] namely, the $f_2(1720)[\theta(1690)]$, $f_2(2010)$, $f_2(2300)$, and $f_2(2340)$, correspond to linear combinations of these four gg states.[59] Liu[58] and Narison[58] have also given arguments favoring the interpretation of $f_2(1720)$ and $f_0(1590)$ [$G(1590)$] as tensor and scalar glueballs, respectively. In any case, the main 2^{++} gg strength is anticipated[58] and probably observed[22] in the 2–2.2-GeV region, so it is unlikely that the $X_2(1565)$ contains a large gg admixture.

The $Q\bar{Q}g$ hybrid spectrum has been calculated in the bag model,[3,4] the flux tube model,[5] via QCD sum rules,[60] and on the QCD lattice.[61] Although $J^{\pi C}$ exotic states [1^{-+}] are predicted in the mass region of 1.3–1.9 GeV, there are no $2^{++}(0^+)$ states in the $Q\bar{Q}g$ spectrum below 2 GeV.[58–61] Thus, we cannot attribute any significant component of the $X_2(1565)$ to $Q\bar{Q}g$.

To summarize, the $X_2(1565)$ is a plausible candidate for interpretation as an $\bar{N}N$ bound state in the $^{13}P_2$-$^{13}F_2$ channel, whose strong binding arises as a coherent effect of the tensor force. The $X_2(1250)$ and $X_0(1110)$ states in Table I, if confirmed, would be naturally identified as the 1^{--} and 0^{++} members of the $I=0$ $\bar{N}N$ band, satisfying the interval rule (3.11). Although these states would mix with other multiquark configurations ($Q^2\bar{Q}^2$), they retain a dominantly $\bar{N}N$ character. Accordingly, they are produced rather copiously in $\bar{N}N$ annihilation, but with difficulty in other entrance channels such as $\pi^- p$ or $\gamma\gamma$.

IV. PRODUCTION OF $\bar{N}N$ QUASINUCLEAR STATES

Annihilation reactions of the type $\bar{N}N\to\gamma X$, πX to produce QN bound states X were considered in detail by Dover, Richard, and Zabek,[14] abbreviated here as DRZ. The allowed pionic transitions to the $0^{++}(0^+)$, $1^{--}(0^-)$, and $2^{++}(0^+)$ $\bar{N}N$ states $X_{0,1,2}$ are tabulated in Table II.

TABLE II. Allowed transitions $\bar{p}p(^{2I+1,2S+1}L_J)\to\pi^0X_J$.

Initial $\bar{N}N$ state	Final state[a]
$^{31}S_0$	$\pi^0X_0(l=0)$, $\pi^0X_2(l=2)$
$^{33}S_1$-$^{33}D_1$	$\pi^0X_1(l=1)$
$^{33}P_1$	$\pi^0X_0(l=1)$, $\pi^0X_2(l=1,3)$
$^{33}P_2$	$\pi^0X_2(l=1,3)$
$^{31}P_1$	$\pi^0X_1(l=0,2)$

[a]The meson-meson relative orbital angular momentum is denoted by l.

Transitions to the $3^{--}(0^-)$ state X_3 via pion emission are likely to be energetically forbidden (see Fig. 2), but, if X_3 is bound, we can have

$$\bar{p}p(^{13}P_2\text{-}^{33}P_2)\to\gamma X_3(l=1)\ . \tag{4.1}$$

This is a favored $E1$ transition, whereas production of X_3 from $\bar{N}N(L=0)$ will be strongly suppressed because both $E1$ and $M1$ transitions are forbidden. Since X_3 and other X_J's are broad states ($\Gamma\geq 100$ MeV), studies of the inclusive γ spectrum are unlikely to reveal their existence. We consider exclusive reactions in Sec. V, in connection with our discussion of the decay modes of the X_J.

We now focus on the formation of $X_2(1565)$. Define the branching ratio B, averaged over initial states i of spin J_i, as

$$B(\bar{p}p\to\pi^0X_J)=\sum_i(2J_i+1)(\Gamma_\pi^{i\to J}/\Gamma_T^i)\Big/\sum_i(2J_i+1)\ , \tag{4.2}$$

where $\Gamma_\pi^{i\to J}$ is the partial width for the π^0X_J final state and Γ_T^i is the total width of $\bar{N}N$ level i given by

$$\Gamma_T^i=\Gamma_A^i+\sum_f(\Gamma_\pi^{i\to f}+\Gamma_\gamma^{i\to f})\ , \tag{4.3}$$

where Γ_A^i is calculated from Eq. (3.4). In DRZ, a value $v\sigma_A=8$ mb was chosen, in order to produce widths $\Gamma_T^i\approx 20$ MeV for QN states, motivated by the evidence for narrow structures[62] allegedly seen in the $\bar{p}p\to\gamma X$ inclusive spectrum. These narrow "baryonium" candidates have since disappeared,[16–18] and the QN states X_J under discussion here have widths $\Gamma_T\approx 100$–200 MeV, which motivates the choice $v\sigma_A=40$ mb as per Eqs. (3.4)–(3.6). This implies that the DRZ estimates of $B(\bar{p}p\to\pi^0X_J)$ have to be divided by a factor of 5 to account for the increase in $v\sigma_A$. In addition, these predictions have to be adjusted to account for the correct phase space. We adopt a phase-space (PS) factor

$$\mathrm{PS}(q)=C(qR)^{2l+1}\exp(-\alpha q^2R^2)\ , \tag{4.4}$$

where $R=0.8$ fm is a typical hadron radius and the exponential factor arises from overlaps of quark wave functions (see Ref. 38, for which $\alpha\approx 0.23$) or as a consequence of "nearest threshold dominance," as in the statistical model analysis of $\bar{N}N$ annihilation due to Vandermeulen.[63]

The predicted branching ratios for $\bar{N}N\to\pi X_J$ transitions depend on the degree of isospin mixing in the initial atomic state; i.e., there can be strong $\bar{p}p$-$\bar{n}n$ mixing at short distances.[14] For $\bar{N}N(L=0)$, the sensitivity to isospin mixing is particularly acute. Using the formalism of DRZ,[14] with $v\sigma_A=40$ mb and the corrected phase space, we predict

$$B(\bar{p}p(L=0)\to\pi^0X_2)\approx\begin{cases}6.4\times10^{-3} & \text{(Coulomb)},\\ 2.2\times10^{-5} & \text{(mixed)},\end{cases} \tag{4.5}$$

where by "$\bar{p}p(L=0)$," we denote either a pure $\bar{p}p$ wave function ("Coulomb") or a full wave function ("mixed") incorporating $\bar{p}p$-$\bar{n}n$ mixing. For $L=1$, the predictions are much more stable:

$$B(\bar{p}p(L=1)\to\pi^0 X_2)=\begin{cases}4.9\times10^{-2} & \text{(Coulomb)},\\ 3\times10^{-2} & \text{(mixed)}.\end{cases} \tag{4.6}$$

Using the estimate $B(X_2\to\pi\pi)\approx0.2$ from Sec. V, we obtain (for "mixed")

$$B(\bar{p}p(L=1)\to\pi^0 X_2)B(X_2\to\pi\pi)\approx6\times10^{-3}\ , \tag{4.7}$$

which compares very well with the experimental value[29] of Eq. (2.2). For $L=0$, our "Coulomb" prediction is

$$B(\bar{p}p(L=0)\to\pi^0 X_2)B(X_2\to\pi\pi)\approx1.3\times10^{-3}\ ,$$

which is not far from the experimental result[25] obtained from Eq. (2.3). The isospin interference effect predicted (in the Paris model) to suppress the $L=0$ production rate of X_2 is apparently not seen in the data. This suppression is sensitive to the position of the zero in the $^3S_0$ part of the atomic wave function, which, in turn, reflects the (unknown) binding energy of the QN $^3S_0$ state. In the Paris potential model used in Ref. 14, there is no strongly bound $^1S_0$ QN state, so the corresponding quasiatomic state does *not* have a node at short distances of the order of 1 fm. The presence of a node in the $^3S_0$, but not the $^1S_0$, atomic wave function accounts for the large suppression factor due to isospin mixing [Eq. (4.5)] for a transition to an $I=1$ final state. In most other potential models, there exist $^1S_0$ QN bound states,[13] and the value of

$$B(\bar{p}p(L=0)\to\pi^0 X_2)$$

could even be enhanced with respect to the pure Coulomb limit. Without any experimental constraints on the binding energies of the $^1S_0$ and $^3S_0$ QN states, we cannot make any quantitative statement as to the magnitude of $B(\bar{p}p(L=0)\to\pi^0 X_2)$. It does seem likely, however, that a scenario with a bound $^3S_0$ and an unbound $^1S_0$ $\bar{N}N$ state is unacceptable, in that a large (and unobserved) isospin interference effect is predicted in the πX_2 annihilation channel.

From Eqs. (2.2) and (2.3a) and the assumption of a pure $\bar{p}p$ wave function, we obtain

$$\frac{B(\bar{p}p(L=0)\to\pi^0 X_2)}{B(\bar{p}p(L=1)\to\pi^0 X_2)}\approx0.35^{+0.13}_{-0.10}\ . \tag{4.8}$$

Note that if we used Eq. (2.4), this ratio increases to 0.84. Using the Coulomb value for $L=0$, we predict

$$\frac{B(\bar{p}p(L=0)\to\pi^0 X_2)}{B(\bar{p}p(L=1)\to\pi^0 X_2)}\approx0.13\text{–}0.21 \tag{4.9}$$

for the range of values indicated by Eq. (4.6), in rough agreement with experiment. Most of the predicted suppression for $L=0$ is due to kinematics, i.e., the $(L=1)\to(l=1)$ transition is better matched than $(L=0)\to(l=2)$.

Another useful ratio to study is $\pi f_2(1270)/\pi X_2(1565)$. From the $\bar{N}N\to3\pi$ data, using

$$B(f_2(1270)\to\pi^+\pi^-)\approx0.57\ ,$$

we obtain

$$\begin{aligned}R_0B(X_2\to\pi\pi)&=\frac{B(\bar{p}n(L=0)\to\pi^- X_2)B(X_2\to\pi\pi)}{B(\bar{p}n(L=0)\to\pi^- f_2)}\\&\approx5.7\times10^{-2}\ ,\\ R_1B(X_2\to\pi\pi)&=\frac{B(\bar{p}p(L=1)\to\pi^0 X_2)B(X_2\to\pi\pi)}{B(\bar{p}p(L=1)\to\pi^0 f_2)}\\&\approx5.3\times10^{-1}\ .\end{aligned} \tag{4.10}$$

Taking the ratio, we find

$$\frac{R_0}{R_1}\approx\tfrac{1}{10}\ . \tag{4.11}$$

Thus, relative to πf_2, the production of $X_2(1565)$ is enhanced by an order of magnitude from the $\bar{N}N$ p wave. If the ratio (4.11) depended only on kinematical factors, as per Eq. (4.4), and not on spin-flavor weights, we would expect $R_0/R_1\approx1/4$.

In obtaining Eq. (4.7), we assumed $B(X_2\to\pi\pi)\approx0.2$. However, if we take the data[26,27] on X_2 production in the $\rho\rho$ channel at face value, we obtain the limit (2.7) on $B(X_2\to\pi\pi)$ and hence the prediction

$$B(\bar{p}p(L=1)\to\pi X_2)B(X_2\to\pi\pi)\le10^{-3} \tag{4.12}$$

in disagreement with the ASTERIX value of Eq. (2.2). This could imply that the $2^{++}(0^+)$ structures seen in $\pi\pi$ and $\rho\rho$ are *not* the same object. Alternatively, Bridges *et al.*[26,27] are likely to have overestimated the fraction of $\bar{p}n\to3\pi^-2\pi^+$ events attributable to $\bar{p}n\to\pi^- X_2$, which they give as 0.82. For instance, QTB modes such as $\bar{p}n\to\rho^0 A_1^-(l=0)$ have a substantial spin-flavor weight in the quark model,[38] and could give a substantial background. Also, a large contribution from $L=1$ $\bar{p}n$ annihilations, as suggested by Reifenröther and Klempt,[42] could be responsible for the apparent inconsistency of Eq. (4.12). The very large ratio of $\rho\rho$ and $\pi\pi$ decays, as per Eq. (2.7), is not predicted in a microscopic model of QN bound-state decays, as shown in the next section. Note, however, that the $\rho\rho$ decay mode of the $2^{++}(0^+)$ QN state is expected to be larger than the $\pi\pi$ mode by a factor of 2 or so.

V. DECAY MODES OF $\bar{N}N$ BOUND STATES

There have been a number of attempts to describe $\bar{N}N$ annihilation at rest and in flight in terms of a microscopic quark model. Major efforts have been devoted to this problem by the Helsinki,[53,64] Osaka,[65] and Tübingen[38,39,66] groups, among others.[67–69] To calculate decays of $\bar{N}N$ bound states into two mesons, we adopt the annihilation topology $A2$ as shown in Fig. 4. This was suggested as a dominant process in Ref. 67 and exploited systematically in Maruyama, Furui, and Faessler (MFF),[38] together with a direct $\bar{N}N\to M_1M_2M_3$ three-meson reaction, to achieve a good description of $\bar{N}N$ annihilation data over a range of energies.[38–40] The effective $Q\bar{Q}$ annihilation-creation operator has the quantum numbers of the vacuum ($^3P_0$, $I=0$, color singlet).

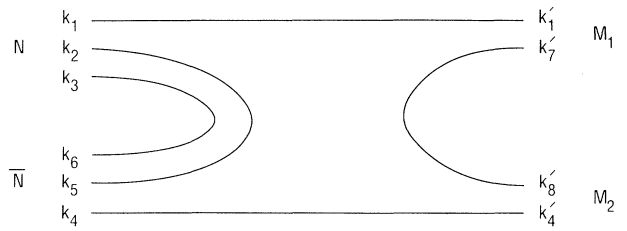

FIG. 4. Mechanism for the decay of the $\bar{N}N$ quasinuclear state into two meson channels M_1+M_2. The $Q\bar{Q}$ pairs are created or annihilated with vacuum quantum numbers $[0^{++}(0^+)]$. The spin-flavor factors for this process are given in Tables IV–VI.

Meson and baryon resonance decays are well described phenomenologically[37] using such an effective $Q\bar{Q}$ vertex; this approximation has been given a basis in strong-coupling QCD.[74,75] Since the $\bar{N}N$ systems considered here share the quantum numbers of a $Q\bar{Q}$ pair, differing only in mass and internal quark composition, it is reasonable to apply the $^3P_0$ model to describe the decays of bound $\bar{N}N$ QN states.

Consider the possible transitions from $L=0,1$ $\bar{N}N$ states to QTB final states M_1M_2. The processes allowed by conservation of $\{J,\pi,C,I,G\}$ are labeled by Y in Table III. In the $^3P_0$ model (Fig. 4), one can attach a spin-flavor (SF) weight to each entry in Table III. For the 0^{++}, 1^{--}, 2^{++} $(I=0)$ states X_J discussed in Secs. II–IV, the values of SF are tabulated in Tables IV–VI, taken from MFF.[38] We also include *sp* decay modes with $s\neq\pi$, although these are generally forbidden or very small because of energy conservation. The s mesons are $\{\pi,\eta,\eta',\rho,\omega,\phi\}$; the p mesons are $\sigma[0^{++}(0^+)]$,

$$\delta=a_0(980)[0^{++}(1^-)]\ ,$$
$$H=h_1(1170)[1^{+-}(0^-)]\ ,$$
$$B=b_1(1235)[1^{+-}(1^+)]\ ,$$
$$A_1=a_1(1260)[1^{++}(1^-)]\ ,$$
$$f=f_2(1270)[2^{++}(0^+)]\ ,$$
$$D=f_1(1285)[1^{++}(0^+)]\ ,$$
$$A_2=a_2(1320)[2^{++}(1^-)]\ .$$

To obtain decay widths, we multiply the weights SF by an appropriate kinematical factor, i.e.,

$$\Gamma=CqF(q)\cdot\mathrm{SF}\cdot(\tfrac{1}{2})^n\cdot(\alpha)^{2n_1}\cdot(\beta)^{2n_2}\ , \tag{5.1}$$

where C is a constant which depends on the quantum numbers of the initial $\bar{N}N$ state, q is the c.m. momentum of either of the mesons, and $F(q)$ is proportional to the absolute square of the amplitudes $\hat{\mathbf{T}}_{A2}$ for $\bar{N}N\to M_1M_2$ transitions obtained by MFF.[38] The factor $(\frac{1}{2})^n$ is applied for modes containing n pions, and roughly represents the spectroscopic factor for the pion as a $Q\bar{Q}$ state.[38,64]

In Tables IV–VI, for modes containing an η or η', the factor SF refers to the production of the flavor combination $\eta_{ud}=(u\bar{u}+d\bar{d})/\sqrt{2}$. The physical η and η' mesons, in the absence of gluonic components, are given by the linear combinations

$$\eta=\alpha\eta_{ud}-\beta\eta_s\ ,$$
$$\eta'=\beta\eta_{ud}+\alpha\eta_s\ , \tag{5.2}$$

TABLE III. Allowed nonstrange decay modes of neutral $\bar{N}N$ quasinuclear states. The notation is as follows: $Y(l)$ is a transition allowed by $J^{\pi C}(I^G)$ conservation with meson-meson orbital angular momentum l; N is a forbidden transition. If $\pm$ occurs, the neutral mode $M_1^0M_2^0$ is forbidden by C parity, but the charged modes $M_1^{\pm}M_2^{\mp}$ are allowed. Note also that the transitions $^{13}P_1\to\rho^+\rho^-$, $\rho^0\rho^0$, and $\omega\omega$ are forbidden by Bose-Einstein statistics. We include *ss* and πp modes, where $S=\{\pi,\eta,\rho,\omega\}$ and $p=\{\sigma,\delta,H,B,A_1,f,A_2\}$; η stands for $\{\eta,\eta'\}$, ω for $\{\omega,\phi\}$, etc.

	$^{11}S_0$	$^{31}S_0$	$^{13}S_1$	$^{33}S_1$	$^{11}P_1$	$^{31}P_1$	$^{13}P_0$	$^{33}P_0$	$^{13}P_1$	$^{33}P_1$	$^{13}P_2$	$^{33}P_2$
$\pi\pi$	N	N	N	$Y(\pm,1)$	N	N	$Y(0)$	N	N	N	$Y(2)$	N
$\pi^0\eta$	N	N	N	N	N	N	N	$Y(0)$	N	N	N	$Y(2)$
$\eta\eta$	N	N	N	N	N	N	$Y(0)$	N	N	N	$Y(2)$	N
$\rho\rho$	$Y(1)$	N	N	$Y(\pm,1)$	N	$Y(\pm,0,2)$	$Y(0,2)$	N	N	N	$Y(0,2)$	N
$\rho^0\omega$	N	$Y(1)$	N	N	N	N	N	$Y(0,2)$	N	$Y(0,2)$	N	$Y(0,2)$
$\omega\omega$	$Y(1)$	N	N	N	N	N	$Y(0,2)$	N	N	N	$Y(0,2)$	N
$\pi\rho$	N	$Y(\pm,1)$	$Y(1)$	N	$Y(0,2)$	N	N	N	N	$Y(\pm,0,2)$	N	$Y(\pm,2)$
$\pi^0\omega$	N	N	N	$Y(1)$	N	$Y(0,2)$	N	N	N	N	N	N
$\eta\rho^0$	N	N	N	$Y(1)$	N	$Y(0,2)$	N	N	N	N	N	N
$\eta\omega$	N	N	$Y(1)$	N	$Y(0,2)$	N	N	N	N	N	N	N
$\pi^0\sigma$	N	$Y(0)$	N	N	N	N	N	N	N	$Y(1)$	N	N
$\pi\delta$	$Y(0)$	N	N	N	N	$Y(\pm,1)$	N	N	$Y(1)$	N	N	N
π^0H	N	N	N	$Y(0,2)$	N	$Y(1)$	N	N	N	N	N	N
πB	N	N	$Y(0,2)$	N	$Y(1)$	N	N	$Y(\pm,1)$	N	$Y(\pm,1)$	N	$Y(\pm,1)$
π^0D	N	N	N	N	N	N	N	$Y(1)$	N	$Y(1)$	N	$Y(1)$
πA_1	N	N	N	$Y(\pm,0,2)$	N	$Y(\pm,1)$	$Y(1)$	N	$Y(1)$	N	$Y(1)$	N
π^0f	N	$Y(2)$	N	N	N	N	N	N	N	$Y(1)$	N	$Y(1)$
πA_2	$Y(2)$	N	N	$Y(\pm,2)$	N	$Y(\pm,1)$	N	N	$Y(1)$	N	$Y(1)$	N

TABLE IV. Spin-flavor (SF) weights for the decay $\bar{N}N(^{13}P_0)\to M_1M_2$. These are relative weights obtained from MFF (Ref. 38) by dividing by 225. We sum over charge states, i.e., $\pi\pi\equiv\pi^0\pi^0+\pi^+\pi^-$, $\pi A_1=\pi^0 A_1^0+\pi^+ A_1^-+\pi^- A_1^+$, etc. We consider $l=0,1,2$ for the orbital angular momentum of the M_1M_2 final state.

Decay channel	SF
$\pi\pi(l=0)$	$\frac{3}{4}$
$\eta\eta(l=0)$	$\frac{1}{4}$
$\rho\rho(l=0)$	$\frac{1}{4}$
$\rho\rho(l=2)$	2
$\omega\omega(l=0)$	$\frac{1}{12}$
$\omega\omega(l=2)$	$\frac{2}{3}$
$\pi A_1(l=1)$	1
$\eta D(l=1)$	$\frac{1}{3}$
$\omega H(l=1)$	$\frac{1}{3}$
$\rho B(l=1)$	1

TABLE VI. Spin-flavor (SF) weights for the decay $\bar{N}N(^{13}P_2)\to M_1M_2$. We divide the weights given by MFF (Ref. 38) by 81.

Decay channel	SF
$\pi\pi(l=2)$	$\frac{3}{10}$
$\eta\eta(l=2)$	$\frac{1}{10}$
$\rho\rho(l=0)$	1
$\rho\rho(l=2)$	$\frac{4}{5}$
$\omega\omega(l=0)$	$\frac{1}{3}$
$\omega\omega(l=2)$	$\frac{4}{15}$
$\pi A_1(l=1)$	$\frac{1}{4}$
$\pi A_2(l=1)$	$\frac{3}{4}$
$\eta D(l=1)$	$\frac{1}{12}$
$\eta f(l=1)$	$\frac{1}{4}$
$\omega H(l=1)$	$\frac{1}{3}$
$\rho B(l=1)$	1

where $\eta_s=s\bar{s}$ is the strange-quark component, and α and β are given in terms of the pseudoscalar mixing angle θ by

$$\alpha=\sqrt{\tfrac{1}{3}}\cos\theta-\sqrt{\tfrac{2}{3}}\sin\theta\ ,$$
$$\beta=\sqrt{\tfrac{1}{3}}\cos\theta+\sqrt{\tfrac{2}{3}}\sin\theta\ . \tag{5.3}$$

In Eq. (5.1), n_1 and n_2 refer to the number of η or η' mesons, respectively. For the calculations displayed in Figs. 5–10, we adopt the canonical value $\theta=-10.7°$ obtained from the quadratic mass formula; in this case $\alpha\approx\beta\approx 1/\sqrt{2}$. More recent decay analyses[71] suggest $\theta\approx -20°$, for which $\alpha\approx 0.82$, $\beta\approx 0.57$. An intermediate value $\theta\approx -14°$ was given by Bramon and Scadron[72] from an analysis which incorporated SU(3) breaking. Thus, the weight α^2 for an η meson [Eq. (5.1)] may vary from $\frac{1}{2}(\theta=-10.7°)$ to $\frac{2}{3}(\theta=-20°)$. Note that we assume that the initial quasinuclear bound state contains no strange quarks ($\Lambda\bar{\Lambda}$ admixtures, $\bar{s}s$ pairs in the nucleon wave function, etc.) and hence the η_s component is not produced. In principle, if the initial state has some $s\bar{s}$ con-

TABLE V. Spin-flavor (SF) weights for the decay $\bar{N}N(^{13}S_1)\to M_1M_2$. We divide the weights given by MFF (Ref. 38) by 25. Some transitions which are allowed by $J^{\pi C}(I^G)$ are forbidden by the dynamics of the $^3P_0$ model; these are $\bar{N}N(^3S_1)\to\rho A_2(l=0)$, $\omega f(l=0)$, $\rho\delta(l=2)$, $\omega\sigma(l=2)$.

Decay channel	SF
$\pi\rho(l=1)$	1
$\eta\omega(l=1)$	$\frac{1}{3}$
$\pi B(l=0)$	$\frac{1}{2}$
$\pi B(l=2)$	1
$\eta H(l=0)$	$\frac{1}{6}$
$\eta H(l=2)$	$\frac{1}{3}$
$\omega\sigma(l=0)$	$\frac{1}{2}$
$\omega D(l=0)$	$\frac{2}{3}$
$\omega D(l=2)$	$\frac{1}{3}$
$\omega f(l=2)$	2
$\rho\delta(l=0)$	$\frac{3}{2}$
$\rho A_1(l=0)$	2
$\rho A_1(l=2)$	1
$\rho A_2(l=2)$	6

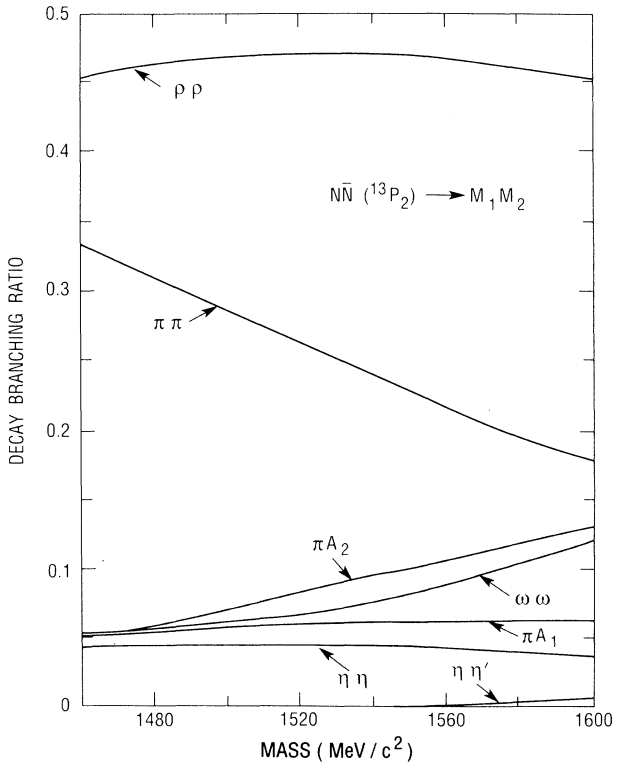

FIG. 5. Branching ratios for the decay of the $2^{++}(0^+)$ quasinuclear $\bar{N}N$ bound state into two meson final states, as a function of its mass. The decay mechanism of Fig. 4 is assumed, with $^3P_0$ $Q\bar{Q}$ vertices. The effects of meson widths are taken into account via Eq. (5.3), and strange-particle decay modes are neglected.

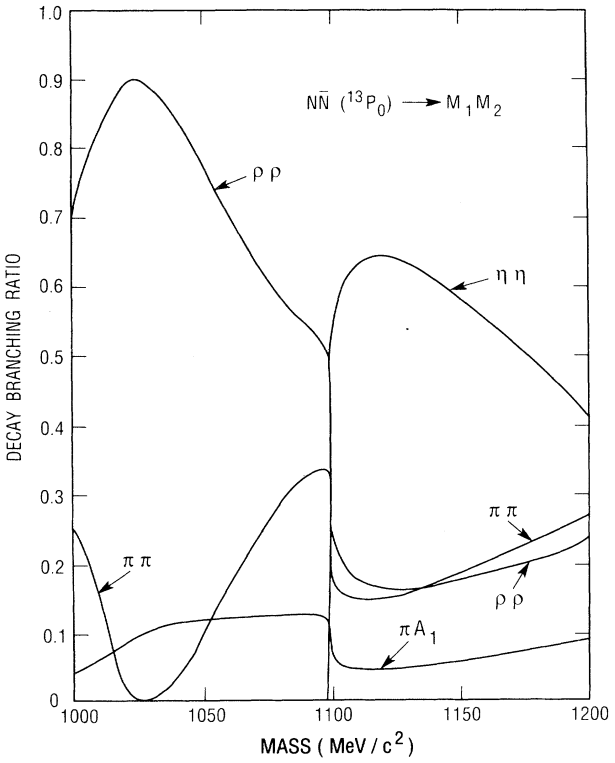

FIG. 6. Two-meson decays for a $0^{++}(0^+)$ $\bar{N}N$ bound state.

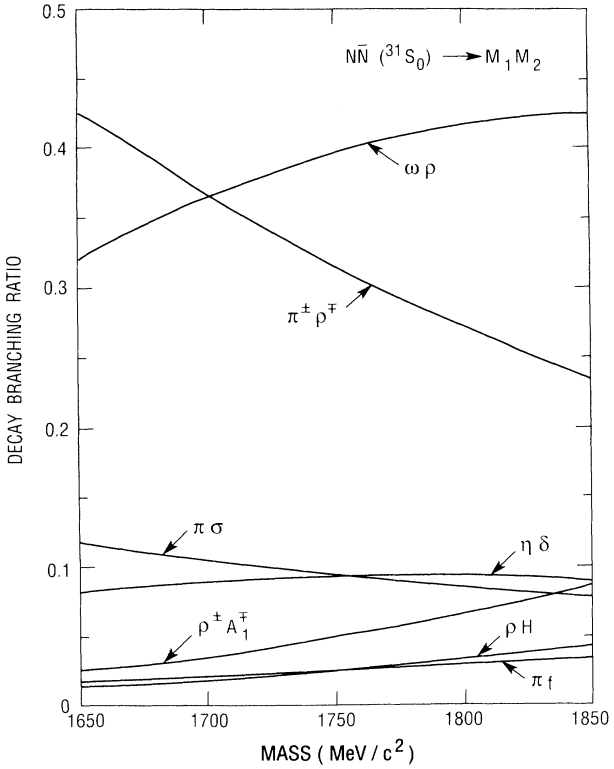

FIG. 8. Two-meson decays for a $0^{-+}(1^-)$ $\bar{N}N$ bound state.

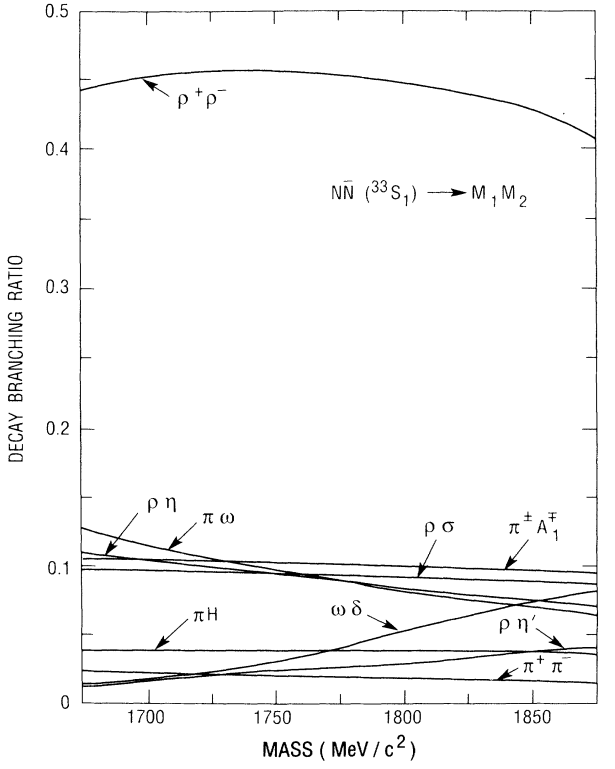

FIG. 7. Two-meson decays for a $1^{--}(1^+)$ $\bar{N}N$ bound state.

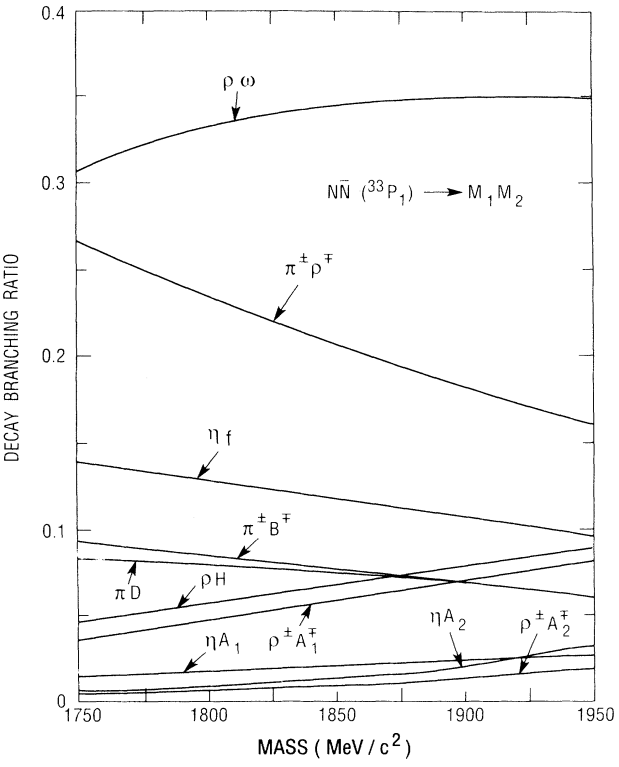

FIG. 9. Two-meson decays for a $1^{++}(1^-)$ $\bar{N}N$ bound state.

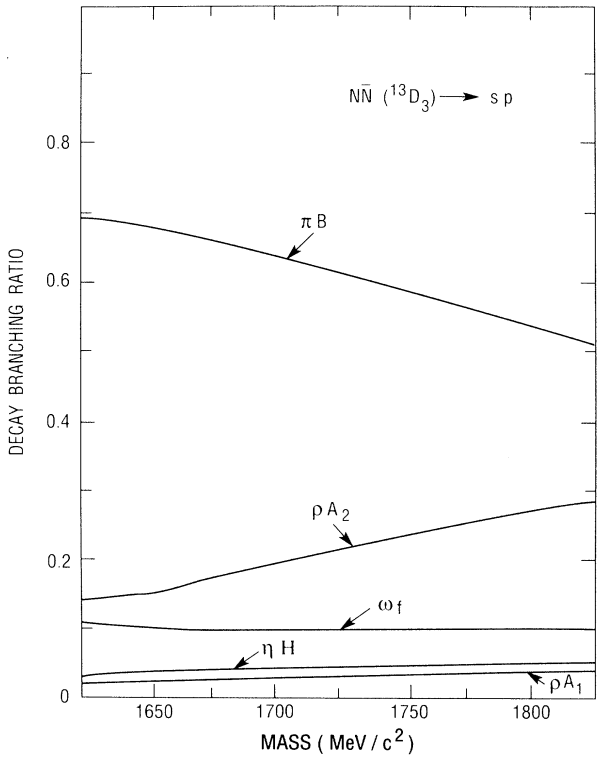

FIG. 10. Relative branching ratios for the decay of a $3^{--}(0^-)$ quasinuclear $\bar{N}N$ bound state into an s meson and a p meson with $l=2$. Decay modes of type $ss(l=3)$ have not been included.

tent, there could be interesting interference effects between η_s and η_{ud} components in final states containing η or η' mesons.[73] This is beyond the scope of the present study.

For transitions from $L=1$ QN states, we have

$$F(q)=\begin{cases}\xi^2(1-x/\xi)^2e^{-z} & \text{for } L=1\to ss(l=0),\\ 6xe^{-z} & \text{for } L=1\to sp(l=1),\\ x^2e^{-z} & \text{for } L=1\to ss(l=2),\end{cases} \tag{5.4}$$

where $x=(qR_M)^2$, $y=R_N^2/R_M^2$, $z=xy/2(y+\frac{2}{3})$, $\xi=3(y+\frac{2}{3})/(y+\frac{1}{3})$, and $\{R_M,R_N\}$ are the meson and nucleon radius parameters, respectively. Transition amplitudes for decays from $L=0$ and 2 QN states are given in Ref. 38. We use $R_N=3.1$ GeV^{-1}, $R_M=4.1$ GeV^{-1} as in Ref. 38, corresponding to rms radii of 0.5 and 0.61 fm for mesons and nucleons, respectively. For broad mesons, we average over the mass spectrum $f(\mu)$:

$$\langle qF(q)\rangle=\int d\mu_1 f_1(\mu_1)\int d\mu_2 f_2(\mu_2)qF(q)\ ,$$
$$f_i(\mu)=\text{const}\times\frac{(\Gamma_i/2)^2}{(\mu-M_i)^2+(\Gamma_i/2)^2}\ , \tag{5.5}$$

where a proper threshold cutoff is introduced as in Ref. 38. For ρ and ω, the spectral function $f(\mu)$ is fitted to the experimental data. We follow the prescription of Nagels *et al.*[76] in parametrizing the mass distribution of the scalar σ meson ($M=760$ MeV, $\Gamma=640$ MeV).

For the decay of the $2^{++}(0^+)$ QN state $X_2(1565)$, the predicted branching ratios are shown in Table VII. Because of phase-space factors, the relative branching ratios depend strongly on the mass M of the $\bar{N}N$ bound state. This dependence is displayed in Figs. 5–10 for the $^{13}P_0$, $^{13}P_2$-$^{13}F_2$, $^{13}D_3$-$^{13}G_3$ members of the $I=0$ band, plus the $^{31}S_0$, $^{33}S_1$-$^{33}D_1$, and $^{33}P_1$ states with $I=1$ which may occur around the $\bar{N}N$ threshold (see Fig. 2).

The dependence of the $2^{++}(0^+)$ decay branching ratios B on the choice of geometrical parameters $\{R_N,R_M\}$ is shown in Table VIII. Within a factor of 2, the values of B remain stable. The $\rho\rho$ mode remains the largest branch, followed by $\pi\pi$. The balance between s- and d-wave $\rho\rho$ decays displays some sensitivity to the choice of $\{R_N,R_M\}$, however. From Eq. (5.2), we have

$$\frac{B(X_2\to\rho\rho(l=0))}{B(X_2\to\rho\rho(l=2))}=\frac{\xi^2(1-x/\xi)^2}{x^2}\ . \tag{5.6}$$

The position of the zero in the numerator depends on $\{R_N,R_M\}$; for our standard choice $\{3.1,4.1\ \text{GeV}^{-1}\}$, we have a zero for $q=0.494$ GeV/c, or $m_\rho=0.607$ GeV/c^2. In our average over the ρ mass spectrum [Eq. (5.5)], we sweep through this point. For smaller $\{R_N,R_M\}$, the zero in $B(X_2\to\rho\rho(l=0))$ receives less weight, and s-wave decay dominates, as one might naively expect for the decay of the $AX(1565)$.

The zero in the amplitude for $L=1\to ss(l=0)$ decays (s refers to an s-wave $\bar{Q}Q$ meson) has a dramatic influence on the relative branching ratios for the decay of the $0^{++}(0^+)$ quasinuclear state, as seen in Fig. 6. The $\pi\pi$ rate is seen to vanish at an X_0 mass of about 1030 MeV, a result which is quite sensitive to the choice of $\{R_N,R_M\}$.

From Table VII, we see that $X_2(1565)$ decay is likely to occur at a measurable level to several final states, including $\eta\eta$, which is accessible with the Crystal Barrel detector at CERN. The $\rho\rho$ channel is predicted to be the largest, but it does not dominate over $\pi\pi$ to the extent suggested by Eq. (2.7). Nevertheless, with the value $B(X_2\to\pi\pi)\approx 0.2$, we predict a production rate of X_2 in $\bar{p}p\to\pi^0\pi^+\pi^-$ events which agrees very well [see Eq. (4.7)] with the ASTERIX result.[29] Thus, the interpretation of $X_2(1565)$ as a quasinuclear $\bar{N}N$ bound state is supported.

TABLE VII. Branching ratios B for $X_2(1565)\to M_1M_2$ decays. The values of B shown are summed over charge states and l. The results for B without and with parentheses refer to a choice $\theta=-10.7°$, $-20°$, respectively, for the pseudoscalar mixing angle.

Channel M_1M_2	$B(X_2(1565)\to M_1M_2)$
$\pi\pi(l=2)$	0.213 (0.208)
$\eta\eta(l=2)$	0.042 (0.073)
$\eta\eta'(l=2)$	0.002 (0.002)
$\rho\rho(l=0,2)$	0.467 (0.456)
$\omega\omega(l=0,2)$	0.093 (0.091)
$\pi A_1(l=1)$	0.063 (0.061)
$\pi A_2(l=1)$	0.112 (0.109)

TABLE VIII. Dependence of branching ratios (for decay of a meson with mass 1565 MeV/c^2) for $2^{++}(0^+)$ decay on size parameters of the nucleon (R_N) and meson (R_M).

R_N (GeV^{-1})	2.5	3.1	3.6	2.5	3.1
R_M (GeV^{-1})	4.1	4.1	4.1	2.8	2.8
$\pi\pi(l=2)$	0.270	0.213	0.176	0.150	0.141
$\rho\rho(l=0)$	0.230	0.231	0.231	0.498	0.480
$\rho\rho(l=2)$	0.218	0.236	0.247	0.088	0.097
$\omega\omega(l=0)$	0.071	0.074	0.076	0.120	0.120
$\omega\omega(l=2)$	0.016	0.019	0.020	0.006	0.007
$\eta\eta(l=2)$	0.042	0.042	0.042	0.018	0.019
$\eta\eta'(l=2)$	0.001	0.002	0.002	0.004	0.005
$\pi A_1(l=1)$	0.054	0.063	0.069	0.043	0.049
$\pi A_2(l=1)$	0.091	0.112	0.128	0.070	0.080

We have not included strange-particle decay modes because they are usually strongly suppressed. For instance, a suppression factor of $\frac{1}{6}$ is applied for strange modes by Furui and Faessler[66] and by Vandermeulen.[63] This suppression can be attributed to the quantum tunneling of massive $\bar{s}s$ pairs.[75] A recent measurement[77] yielded

$$B(\bar{p}p(L=1)\to K^+K^-)/B(\bar{p}p(L=1)\to\pi^+\pi^-) \approx 0.06\pm0.012 \quad (5.7)$$

at rest. We expect similar ratios for $X_2(1565)$ decays. This agrees with the strong suppression [Eq. (2.5)] seen by Gray *et al.*[25] and further supports the QN picture of $X_2(1565)$. If $X_2(1565)$ were a glueball, for instance, there is no obvious reason for its $\bar{K}K$ decay mode to be suppressed, since it is a "flavor blind" object.

VI. CONCLUSIONS AND KEY EXPERIMENTS

We have argued that there exists a spectroscopy of $\bar{N}N$ quasinuclear bound states which falls outside the usual nonet structure of $Q\bar{Q}$ mesons. These states X_J are optimally formed in $\bar{N}N\to MX_J$ annihilation reactions, where $M=\{\pi,\eta,\rho,\omega\}$. We have presented estimates of the masses, production rates, and decay branching ratios of these QN states. These predictions are consistent with the properties of the $X_2(1565)$, a $2^{++}(0^+)$ meson first seen in the $\bar{p}n\to 2\pi^-\pi^+$ reaction by Gray *et al.*[25] and more recently in $\bar{p}p\to\pi^0\pi^+\pi^-$ by May *et al.*[29] There are also candidates for broad 1^{--} and 0^{++} states from $\bar{p}p\to\pi^0e^+e^-$ and $\bar{p}n\to\rho^-\pi^+\pi^-$ annihilations which could be the lower spin members of the $I=0$ natural-parity band predicted in $\bar{N}N$ potential models. The principal agency for the strong binding of these states is the coherent tensor force generated by pseudoscalar and vector meson exchange. This coherence leads to a strongly attractive $\bar{N}N$ interaction at rather *long range* ($r\gtrsim 1$ fm) for $I=0$, $S=1$, $L=J\pm1$ configurations ($^3P_0$, $^3S_1$-$^3D_1$, $^3P_2$-$^3F_2$, ...). The mass spectrum of these states in a nonrelativistic model assumes the form of a rotational band, with

$$M(J)=M(0)+\Delta M\ J(J+1)\ ,$$

leading to an interval rule quite distinct from that for a Regge trajectory, for instance, for four-quark ($Q^2\bar{Q}^2$) states.

A number of key experiments remain to be done to verify (or disprove) our hypothesis of QN states. To establish the existence of the $1^{--}(0^-)$ quasinuclear state X_1, one would study the production reactions

$$\bar{p}p(L=0,1)\to\pi^0X_1,\eta X_1,\rho^0X_1,\omega X_1(l=1,0)\ .$$

Since X_1 is expected to be deeply bound, all of these processes warrant attention for $\bar{p}p$ annihilation at rest [for $X_2(1565)$, only π^0X_2 is relevant]. For ρ^0X_1 and ωX_1, we would expect $l=0$ to dominate, so these are best explored starting from $L=1$ $\bar{p}p$ atomic states. The strong decay of X_1 proceeds almost entirely into the $\pi\rho$ channel if $M(X_1)\lesssim 1300$ MeV; at higher masses of 1300–1400 MeV, the modes $X_1\to\sigma\omega$, $\eta\omega$ πB enter at the 2–5 % level. If X_1 lies in the same mass region as the $a_2(1320)$, it will be difficult to disentangle its $\pi\rho$ decay from that of the a_2. Note, however, that $a_2\to\pi\rho(l=2)$, whereas $X_1\to\pi\rho(l=1)$, so one could distinguish X_1 from a_2 by an analysis of the decay angular distribution. An alternative would be to look for an electromagnetic decay mode such as $X_1\to\pi^0\gamma$ or $X_1\to e^+e^-$ (for the ω, which has the same quantum numbers as the X_1, the corresponding branching ratios are 8 and 0.007 %, respectively).

Perhaps the most critical measurement is the search for the decay chain $\bar{p}p\to\pi^0X_2(1565)$;

$$X_2(1565)\to\eta\eta(l=2)\ .$$

In this case, the final state contains six photons in about 15% of the events ($\eta\to\gamma\gamma$ is a 39% branch) and is ideally suited to the Crystal Barrel detector at LEAR.

The decay mode $X_2(1566)\to\omega\omega$ should also be observable (see Fig. 5), although it is restricted by the available phase space. In the reaction $\pi^-p\to\omega\omega n$ at 38 GeV/c, the GAMS Collaboration[78] has presented evidence for a pair of $2^{++}(0^+)$ tensor mesons which couple to the $\omega\omega$ system, with masses (1643±7, 1956±20 MeV) and widths (<70 MeV, 220±60 MeV). It is possible that the lower of these states is essentially the upper half of the $X_2(1565)$. Note that the line shape of the $X_2(1565)$, as seen in the $\omega\omega$ channel, will be significantly distorted due to phase space. In the $\bar{N}N$ potential models, there are generally two bound $2^{++}(0^+)$ states in the absence of the

off-diagonal tensor coupling,[32] corresponding to the $^{13}P_2$ and $^{13}F_2$ configurations. When $^{13}P_2$-$^{13}F_2$ tensor coupling is included, one of the states is pushed down in mass, and approximates the coherent mixture X_2 of Eq. (3.8). We have identified this object as the $X_2(1565)$. The second $2^{++}(0^+)$ state which we call X_2', is pushed into the $\bar{N}N$ continuum, and one might (very speculatively) identify it with the $2^{++}(0^+)$ state near 1960 MeV seen by GAMS.[78] This object lies close to the $\bar{N}N$ threshold, and hence its interpretation as a quasinuclear resonance is not unreasonable. Note, however, that a $2^{++}(0^+)$ meson in this mass region could also be interpreted in other ways, for instance, as a $Q^2\bar{Q}^2$ state, a radial excitation of the $f_2(1270)$ meson, a glueball, or a mixture of all these. To shed light on the nature of the $X_2'(1960)$, it is essential to search for $\bar{N}N$ quasinuclear states in the continuum, seen as s-channel resonances in exclusive channels such as $\bar{N}N \to X \to \omega\omega$, $\eta\eta$, $\eta\eta'$, $\bar{K}K$, etc.

Finally, we note that it is important to clarify the nature of the $\pi^+\pi^-$ structure near 1100 MeV (see Table I). In the studies of the $\bar{p}p \to \omega\pi^+\pi^-$ (Ref. 44) and $\bar{p}p \to \rho^0\pi^+\pi^-$ (Ref. 45) reactions, a structure in the $I=0$, $J=0$ $\pi\pi$ system was introduced in order to fit the data. This structure was also seen in $\bar{p}n \to \rho^-\pi^+\pi^-$ (Ref. 30) and there is a hint of it in the $\bar{N}N \to 3\pi$ spectra of Fig. 1. In the context of the $\bar{N}N$ quasinuclear picture, we would like to interpret this structure as the $0^{++}(0^+)$ state X_0, which owes its strong binding to the coherent tensor force. Obviously it is somewhat bold and perhaps foolhardy to interpret an object so far below the $\bar{N}N$ threshold as a quasinuclear $\bar{N}N$ bound state. However, this interpretation has some observable consequences, as seen from Fig. 6. Clearly a search for the $\eta\eta$ and $\pi^0\pi^0$ decay modes of the $X_0(1100)$ is most relevant. Although the line shape in the $\eta\eta$ channel is distorted due to phase space [as for the $\omega\omega$ decay of $X_2(1565)$], the $\eta\eta$ mode should be clearly seen, whereas the $\bar{K}K$ mode is expected to be strongly suppressed, as for $X_2(1565)$ decay. Another promising reaction is $\bar{p}p(^{11}S_0) \to \eta X_0(l=0)$; $X_0 \to \eta\eta$. This signal should appear cleanly in the six-photon final state. Thus, for both the X_0 and X_2 searches, the study of the all neutral final states $3\pi^0$, $\eta\pi^0\pi^0$, $\eta\eta\pi^0$, and 3η is crucial. Such a study would yield the relative branching ratios for the decays $X_{0,2} \to \pi^0\pi^0$, $\eta\eta$, providing a stringent test of the scenario of $\bar{N}N$ quasinuclear states offered here.

ACKNOWLEDGMENTS

The work of C.B.D. was supported in part by a Senior Fellowship of the Alexander von Humboldt Foundation, and T.G. and A.F. were supported by the Deutsche Forschungsgemeinschaft. This manuscript has been authored under Contract No. DE-AC02-76-CH00016 of the U.S. Department of Energy.

[1]R. L. Jaffe, Phys. Rev. D **15**, 267 (1977); **15**, 281 (1977); **17**, 1445 (1978).
[2]Chan Hong Mo and H. Høgaasen, Phys. Lett. **72B**, 121 (1977).
[3]M. Chanowitz and S. Sharpe, Nucl. Phys. **B222**, 211 (1983).
[4]T. Barnes, F. E. Close, and F. de Viron, Nucl. Phys. **B224**, 241 (1983).
[5]N. Isgur, R. Kokoski, and J. Paton, Phys. Rev. Lett. **54**, 869 (1985).
[6]T. Barnes, F. E. Close, and S. Monaghan, Nucl. Phys. **B198**, 380 (1982).
[7]P. M. Fishbane and S. Meshkov, Comments Nucl. Part. Phys. **13**, 325 (1984).
[8]M. Chanowitz, in *Multiparticle Dynamics 1983,* Proceedings of the XIV International Symposium, Lake Tahoe, 1983, edited by P. M. Yager and J. F. Gunion (World-Scientific, Singapore, 1984).
[9]J. F. Donoghue, in *The Quark Structure of Matter,* Proceedings of the Yukon Advanced Study Institute, Canada, 1984, edited by N. Isgur *et al.* (World-Scientific, Singapore, 1985).
[10]O. D. Dalkarov, V. B. Mandelzweig, and I. S. Shapiro, Nucl. Phys. **B21**, 88 (1970).
[11]L. N. Bogdanova, O. D. Dalkarov, and I. S. Shapiro, Ann. Phys. (N.Y.) **84**, 261 (1974); I. S. Shapiro, Phys. Rep. C **35**, 129 (1978).
[12]J. M. Richard, M. Lacombe, and R. Vinh Mau, Phys. Lett. **64B**, 121 (1976).
[13]W. Buck, C. B. Dover, and J. M. Richard, Ann. Phys. (N.Y.) **121**, 47 (1979); C. B. Dover and J. M. Richard, *ibid.* **121**, 70 (1979).
[14]C. B. Dover, J. M. Richard, and M. C. Zabek, Ann. Phys. (N.Y.) **130**, 70 (1980); later calculations by O. V. Maxwell, J. M. Richard, and W. Weise, Nucl. Phys. **A362**, 301 (1981), include effects of initial state annihilation and pion rescattering.
[15]J. Weinstein and N. Isgur, Phys. Rev. Lett. **48**, 659 (1982); Phys. Rev. D **27**, 588 (1983); **41**, 2236 (1990).
[16]A. Angelopoulos *et al.*, Phys. Lett. B **178**, 441 (1986); Nucl. Phys. B (Proc. Suppl.) **8**, 54 (1989); see also, A. Angelopoulos *et al.*, Phys. Lett. B **212**, 129 (1988) for a discussion of the $\bar{p}n$ contribution with $L=1$ in $\bar{p}d$ annihilation.
[17]L. Adiels *et al.*, Phys. Lett. B **182**, 405 (1986).
[18]M. Chiba *et al.*, Phys. Rev. D **36**, 3321 (1987).
[19]G. C. Rossi and G. Veneziano, Phys. Rep. **63**, 149 (1980).
[20]S. I. Bityukov *et al.*, Phys. Lett. B **188**, 383 (1987).
[21]D. Alde *et al.*, Phys. Lett. B **205**, 397 (1988).
[22]A. Etkin *et al.*, Phys. Rev. Lett. **49**, 1620 (1982); Phys. Rev. D **25**, 2446 (1982).
[23]R. S. Longacre *et al.*, Phys. Lett. B **177**, 223 (1986).
[24]D. Alde *et al.*, Nucl. Phys. **B269**, 485 (1986); Phys. Lett. B **182**, 105 (1986).
[25]L. Gray *et al.*, Phys. Rev. D **27**, 307 (1983).
[26]D. Bridges *et al.*, Phys. Rev. Lett. **56**, 211 (1986); **56**, 215 (1986).
[27]D. Bridges, I. Daftari, and T. E. Kalogeropoulos, Phys. Rev. Lett. **57**, 1534 (1986).
[28]S. Ahmad *et al.*, in *Physics at LEAR with Low Energy Antiprotons,* Proceedings of the IVth LEAR Workshop, Villars-sur-Ollon, 1988, edited by C. Amsler *et al.* (Harwood, Chur, 1988), Vol. 14, p. 447.
[29]B. May *et al.*, Phys. Lett. B **225**, 450 (1989); Z. Phys. C **46**, 191 (1990); **46**, 203 (1990).

[30]I. Daftari, L. Gray, T. E. Kalogeropoulos, and J. Roy, Phys. Rev. Lett. **58**, 859 (1987).
[31]K. D. Duch *et al.*, Z. Phys. C **45**, 223 (1989).
[32]C. B. Dover and J. M. Richard, Phys. Rev. D **17**, 1770 (1978).
[33]C. B. Dover, Phys. Rev. Lett. **57**, 1207 (1986).
[34]K. F. Liu and B. A. Li, Phys. Rev. Lett. **58**, 2288 (1987).
[35]S. K. Bose and E. C. G. Sudarshan, Phys. Rev. Lett. **62**, 1445 (1989).
[36]T. Ueda, in *Physics at LEAR with Low Energy Antiprotons* (Ref. 28), p. 453.
[37]A. LeYaouanc *et al.*, Phys. Rev. D **8**, 2223 (1973); **9**, 1415 (1974); **11**, 1272 (1975).
[38]M. Maruyama, S. Furui, and A. Faessler, Nucl. Phys. **A472**, 643 (1987).
[39]M. Maruyama, S. Furui, A. Faessler, and R. Vinh Mau, Nucl. Phys. **A473**, 649 (1987).
[40]T. Gutsche, M. Maruyama, and A. Faessler, Nucl. Phys. **A503**, 737 (1989).
[41]G. Bassompierre *et al.*, Phys. Lett. **65B**, 397 (1976).
[42]J. M Richard and M. E. Sainio, Phys. Lett. **110B**, 349 (1982); J. Carbonell, G. Ihle, and J. M. Richard, Z. Phys. A **334**, 329 (1989); E. Klempt, Phys. Lett. B **244**, 122 (1990); G. Reifenröther and E. Klempt, *ibid.* **245**, 129 (1990).
[43]V. M. Kolybasov, I. S. Shapiro, and Yu. N. Sokolskikh, Phys. Lett. B **222**, 135 (1989).
[44]R. Bizzarri *et al.*, Nucl. Phys. **B14**, 169 (1969).
[45]J. Díaz *et al.*, Nucl. Phys. **B16**, 239 (1970).
[46]K. Königsmann, Phys. Rep. **139**, 243 (1986).
[47]T. A. Armstrong *et al.*, Phys. Lett. B **227**, 186 (1989).
[48]H. Kolanoski, Nucl. Phys. B (Proc. Suppl.) **8**, 41 (1989).
[49]M. Althoff *et al.*, Z. Phys. C **16**, 13 (1982); H. J. Behrend *et al.*, *ibid.* **21**, 205 (1984).
[50]N. N. Achasov *et al.*, Z. Phys. **16**, 55 (1982).
[51]B. A. Li and K. F. Liu, Phys. Rev. D **30**, 613 (1984).
[52]F. Myhrer and A. W. Thomas, Phys. Lett. **64B**, 59 (1976); F. Myhrer and A. Gersten, Nuovo Cimento **37A**, 21 (1977).
[53]J. A. Niskanen and A. M. Green, Nucl. Phys. **A431**, 593 (1984).
[54]B. Moussallam, Doctoral thesis, Université Pierre et Marie Curie, France, 1985 (unpublished).
[55]R. Vinh Mau, in *Medium Energy Nucleon and Antinucleon Scattering,* Vol. 243 of *Lecture Notes in Physics,* edited by H. V. von Geramb (Springer-Verlag, Berlin, 1985), pp. 3–23, see especially Table 7; R. Vinh Mau, in *Hadron Structure in Nuclear Physics (Bloomington, Indiana),* Proceedings of the 1983 Indiana University Nuclear Physics Workshop on Manifestations of Hadron Substructure in Nuclear Physics, AIP Conf. Proc. No. 110, edited by W-Y. P. Hwang and M. H. Macfarlane (AIP, New York, 1983), p. 187.
[56]M. Lacombe, B. Loiseau, B. Moussallam, and R. Vinh Mau, Phys. Rev. C **29**, 1800 (1984).
[57]C. B. Dover and S. H. Kahana, Phys. Lett. **62B**, 293 (1976).
[58]*Glueballs, Hybrids and Exotic Hadrons,* AIP Conf. Proc. No. 185, edited by Suh-Urk Chung (AIP, New York, 1989), see the articles by S. Godfrey, K. F. Liu, S. Meshkov, S. Narison, and G. Schierholz.
[59]R. Sinha, S. Okubo, and S. F. Tuan, Phys. Rev. D **35**, 952 (1987).
[60]J. L. LaTorre, P. Pascual, and S. Narison, Z. Phys. C **34**, 347 (1987).
[61]N. A. Campbell, L. A. Griffiths, C. Michael, and P. E. L. Rakow, Phys. Lett. **142B**, 291 (1984).
[62]P. Pavlopoulos, Phys. Lett. **72B**, 415 (1978).
[63]J. Vandermeulen, Z. Phys. C **37**, 563 (1988).
[64]A. M. Green and J. A. Niskanen, Nucl. Phys. **A412**, 448 (1984); **A430**, 605 (1984); **A446**, 543 (1985).
[65]M. Maruyama and T. Ueda, Nucl. Phys. **A364**, 297 (1981); Prog. Theor. Phys. **73**, 1211 (1985); **74**, 526 (1985).
[66]S. Furui, A. Faessler, and S. B. Khadkikar, Nucl. Phys. **A424**, 495 (1984); S. Furui and A. Faessler, *ibid.* **A468**, 669 (1987).
[67]C. B. Dover, P. M. Fishbane, and S. Furui, Phys. Rev. Lett. **57**, 1538 (1986); C. B. Dover and P. M. Fishbane, Nucl. Phys. **B244**, 345 (1984).
[68]E. M. Henley, T. Oka, and J. Vergados, Phys. Lett. **166B**, 274 (1986).
[69]M. Kohno and W. Weise, Nucl. Phys. **A454**, 429 (1986).
[70]C. Amsler, private communication.
[71]F. Gilman and R. Kauffman, Phys. Rev. D **36**, 2761 (1987); N. A. Roe *et al.*, *ibid.* **41**, 17 (1990); H. Aihara *et al.*, Phys. Rev. Lett. **64**, 172 (1990).
[72]A. Bramon and M. D. Scadron, Phys. Lett. B **234**, 346 (1990).
[73]C. B. Dover and P. M. Fishbane, Phys. Rev. Lett. **64**, 3115 (1990).
[74]N. Isgur and J. Paton, Phys. Rev. D **31**, 2910 (1985).
[75]H. G. Dosch and D. Gromes, Phys. Rev. D **33**, 1378 (1986); Z. Phys. C **34**, 139 (1987).
[76]M. Nagels *et al.*, Phys. Rev. D **12**, 744 (1975).
[77]M. Doser *et al.*, Nucl. Phys. **A486**, 493 (1988).
[78]F. G. Binon, in *Glueballs, Hybrids and Exotic Hadrons,* AIP Conf. Proc. No. 185, edited by Suh-Urk Chung (AIP, New York, 1989), p. 135.